

## Effects of Corrosion on the Microstructure, Hardness, and Microhardness of ASTM A335 P92 Steel

Juan Orozco<sup>a,b,\*</sup>, Viatcheslav Kafarov<sup>a</sup>, Dario Peña<sup>b</sup>

<sup>a</sup>Universidad Industrial de Santander, Escuela de Ingeniería Química, Centro de Investigación para el Desarrollo Sostenible en Industria y Energía – CIDES, cra 27 calle 9, Bucaramanga –Santander, Colombia

<sup>b</sup>Universidad Industrial de Santander, Escuela de Ingeniería Metalúrgica y Ciencia de Materiales, Grupo de Investigaciones en Corrosión – GIC, cra 27 calle 9, Bucaramanga –Santander, Colombia  
 ingjorozcoa@gmail.com

In the present work was evaluated the microstructure of ASTM A335 P92 steel when this material is exposed to two corrosive mixtures O<sub>2</sub> - H<sub>2</sub>O, O<sub>2</sub> - N<sub>2</sub> - H<sub>2</sub>O. In addition, the hardness and microhardness of this steel were studied. The equipment used to perform the metallography tests was an Olympus GX 71 microscope. The microhardness tests were performed on an Innovatest 400TM Series microdurometer, 230 V / 50Hz / 3A. The load applied for the microhardness analysis was equal to 50 gf. The hardness tests were performed using a Wilson hardness tester, using an applied load of 60 kgf. The tempered martensite steel microstructure was observed before exposure to corrosive environments. When this material was exposed to corrosive environments, the steel showed changes in its microstructure tending the tempered martensite to transform into a ferritic matrix. Moreover, changes in the microhardness and hardness of the material directly related to the changes in microstructure were observed as a result of the presence of oxides and carbides.

### 1. Introduction

The deterioration of the mechanical properties of the materials implies a reduction in its resistance to thermal creep, thermal fatigue, internal stresses and differences in thermal expansion between the base material and the corrosion products formed (Peña et al., 2014). These decreases in material properties result in equipment failures, causing large economic losses in the industry, mainly due to unexpected production downtime. In addition, this situation implies a high frequency of corrective maintenance and short-term protection, as well as the complete replacement of materials exposed to aggressive atmospheric conditions. According to (Gil De Fuentes, 2013), in the industry, the most important of all operational failures is corrosion, with 33 % of cases. To counteract this situation, materials such as ferritic steels have been developed, which are a series of alloys that favour the increased life of the metal components of the equipment, in addition to being able to operate at higher temperatures each time to achieve greater efficiency. In the conversion of raw materials, which translates into greater profitability in the processes (Peña-Ballesteros et al., 2012). It has been shown that, despite the high temperatures, these steels behave very well in corrosive environments during operations in atmospheres with the presence of air.

Ferritic steel ASTM A335 P92 is a material widely used in the petrochemical industry, in equipment such as boilers, superheaters and heat exchangers. This material is an alloy with excellent structural properties (mainly due to the presence of elements such as V, Mo, Nb, W, among others) has better resistance to thermofluence than most ferritic steels, due to the hardening offered by the addition of tungsten (Barbadikar et al., 2015). However, when ferritic steels are subjected to high temperatures and long periods of time, failures in materials and structures are observed (Gond et al., 1993). It is believed that one of the main reasons why steels with Chromium (9 % Cr) have such high corrosion rates in the presence of combustion gases, is due to the presence of water vapour, which is registered in the literature (Young, 2016). In a study developed by (Carrizo, Besoky, Luppo, Danon, & Ramos, 2018) an ASTM A335 P91 steel was characterized, after applying continuous cooling cycles at moderate rates. It was observed through the characterization techniques of scanning electron microscopy and transmission electron microscopy, phases such as (Fe, Cr)<sub>3</sub>C and V-rich MX in martensite and

$M_2X$  and  $M_{23}C_6$  in the ferrite phase where ( $M = Cr, Fe$ ) and  $MX$  ( $M = Nb, V; X = C, N$ ). This research is part of the set of studies carried out by (Kafarov et al., 2015) where the combustion process was studied by simulation tools and experimentally, in addition, Orozco et al. (2018) proposed a methodology for the analysis of materials exposed to combustion refinery atmospheres; it allowed the kinetic study of the ASTM A335 P92 material, also, this material has been characterised by means of characterization techniques such as X-ray Photoelectron Spectroscopy (XPS), X-ray Diffraction (DRX), Scanning Electron Microscopy (SEM), among others; with the objective of obtaining the corrosive products and understanding the phenomena and mechanisms of corrosion (Orozco et al., 2017). The study contribution focuses on the possibility of observing changes in the microstructure of a material, such as ASTM A335 P92 steel, exposed to corrosive environments from refinery gas combustion processes, as well as determining the correlation among these changes in the microstructure with the effects on properties such as the hardness and microhardness of the materials. At present, there are very few investigations that seek to study the microstructure of ASTM A335 P92 steel and even more scarce, those investigations that contemplate the effect of water vapour within combustion environments. This work aims to be a guide for future research on materials used in the petrochemical industry.

## 2. Methodology

### 2.1 Obtaining study atmospheres and determining variables

The selection of corrosive atmospheres to be evaluated was determined by Orozco et al., 2018. In this study, two combustion gas mixtures were determined in the Barrancabermeja refinery, for the study of oxidation, nitridation and water vapour phenomena. These mixtures can be observed in Tables 1 and 2. Four study temperatures (450 °C, 550 °C, 650 °C and 750 °C), atmospheric pressure (1 atm) and five exposure times (1 h, 20 h, 50 h, 100 h and 200 h) were selected. The ASTM A335 P92 composition can be observed in Table 3.

Table 1: Oxidation-water vapour mixture composition

Compounds	O <sub>2</sub>	H <sub>2</sub> O
% Molar	9.5	90.5

Table 2: Oxidation-nitridation-water vapour mixture composition

Compounds	O <sub>2</sub>	H <sub>2</sub> O	N <sub>2</sub>
% Molar	1.9	18.4	79.7

Table 3: ASTM A335 P92 composition

Element	C	Mn	Si	P	S	Cr	Mo
% weight	0.115	0.454	0.220	0.013	0.0033	9.14	0.4
Element	Ni	Al	V	Nb	W	N	B
% weight	0.119	0.011	0.165	0.055	1.979	0.039	0.022

### 2.2 Manufacture of corrosion coupons

The cutting process of the ASTM A335 P92 steel was carried out by means of the thread cutting technique until a rectangular parallelepiped shape with dimensions of 15 mm long x 10 mm wide x 2 mm thick, with a hole 1mm in the maximum height of 1mm in diameter. The surfaces of the specimens were sanded with 200, 400, 600, 800 and 1,200 silicon carbide sandpaper. Subsequently, the specimens were immersed in acetone by subjecting them to a 10 min ultrasonic bath, with the aim of removing impurities. The above following the ASTM G1-03 standard "Standard Practice for preparing, cleaning, and evaluation of the Corrosion Test Specimens" (ASTM & Environments, 2011).

### 2.3 Analysis of hardness, microhardness and metallographic before the exposition

Before the beginning, the experiments, the hardness and microhardness tests were performed on the ASTM A335 P92 steel, besides observing its microstructure. For these studies, moreover, to the roughing process described above, the diamond paste specimens with particle sizes of 3 µm and 1 µm were polished, following the ASTM E 3-95 standard "Standard Practice for Preparation of Metallographic Specimens" (ASTM, 1995). Also, a chemical attack was carried out on the coupons with Vilella solution (100 mL ethanol, 1g of picric acid and 5 mL of hydrochloric acid) following ASTM E-407-07 "Standard Practice for Microetching Metals and Alloys" (ASTM, 2015). These analyses were effectuated with the collaboration of the steel plant staff of the Industrial University of Santander. The equipment used to perform the metallography tests was an Olympus GX 71 microscope. The microhardness tests were performed on an Innovatest 400TM Series microdurometer, 230 V

/ 50Hz / 3A. The load applied for the microhardness analysis was equal to 50 gf. The hardness tests were performed using a Wilson hardness tester, using an applied load of 60 kgf.

#### 2.4 Exposition of the material with the corrosive atmospheres

ASTM A335 P92 steel was exposed to the two corrosive mixtures where four working temperatures (450 °C, 550 °C, 650 °C and 750 °C), a pressure atmosphere (1 atm) and five exposure times (1 h, 20 h, 50 h, 100 h and 200 h) were evaluated.

#### 2.5 Hardness, microhardness and metallographic analyzes after experimentation

Finally, after exposure of ASTM A335 P92 steel to corrosive oxidation environments - water vapour and nitriding - water vapour, hardness, microhardness, and metallographic analyzes were carried out with the objective of analyzing the changes observed in the material.

### 3. Results

Initially, the micrographs were taken of the steel, before the exposure to the combustion environments, as shown in Figure 1. The initial microstructure of the Steel is a structure of tempered martensite.



Figure 1: a) Micrographs of ASTM A335 P92 steel before exposure to corrosive environments, 100 µm; 1b) Micrographs of ASTM A335 P92 steel before exposure to corrosive environments, 10 µm

#### 3.1 Oxidation-water vapour environment

In Figure 2, it is possible to observe the microstructures of ASTM A335 P92 steel, after the material was exposed to the corrosive oxidation-water vapour environment, for the different working temperatures and 200 h of experimentation.

For the temperatures of 450 °C and 550 °C, the formation of oxides is observed in the material. Moreover, the formation of metal carbides of elements such as W, Mo, V, Nb, and Fe within the steel structure is evident. For the micrographs observed at the temperatures of 650 °C and 750 °C, the tempered martensite tends to transform into a ferritic matrix with carbide precipitation. Moreover, a greater amount of oxides is observed in the material than those observed at lower temperatures (450 and 550 °C). Likewise, there is greater growth and precipitation of carbides, a result of a greater globulisation of these. Also, it is observed that these carbides begin to be located in the grain boundaries of the structure.

In Figure 3a, the variation of the microhardness in the material for the study conditions is observed. It is important to highlight that the steel presented an initial microhardness of 310.9 HV. The load applied for the analyzes was 50 gf. For all working temperatures, an increase in microhardness was evidenced at the first hours of exposure, mainly due to the precipitation of carbides. Depending on the exposure time and operating temperature, a decrease in the microhardness of the steel is evident, especially for the temperature of 750 °C, where the material reached a value of 209 HV. This was the lowest value obtained in the material, decreasing in this way their initial microhardness in a percentage equal to 32.8 %. This is possibly due to the fact that when the maximum design temperature of the material is exceeded (620 °C), the steel increases the speed of the diffusive processes, which allows decreasing the carbon content distributed homogeneously in the matrix, grouping in the limits of grain in form of carbides. The tempered martensite tends to transform with the rise in this temperature and the precipitation of carbides.

In Figure 3b, the behaviour of the hardness in the material is shown. The initial hardness of the steel was 60.2 HRA. It is possible to observe that the material for the working temperatures of 450, 550 and 650 °C do not show a significant variation. This is mainly as a result of the effect of the alloying elements (W), molybdenum (Mo) and vanadium (V), which are carbide forming. However, as observed for the behaviour of the hardness in the material, for the temperature of 750 °C, a decrease was observed up to 55 HRA, which is mainly due to the

increase in temperature, the material experiencing changes, due to that the tempered martensite tends to transform into a stable ferrite matrix with carbide precipitation.

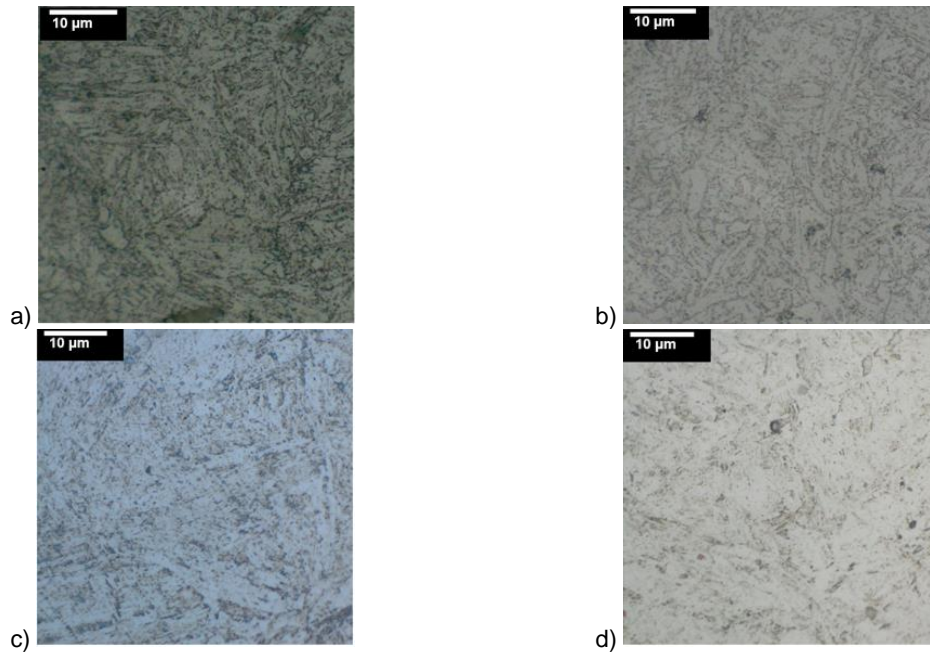


Figure 2: Micrographs of ASTM A335 P92 steel after 200 h of exposure to oxidation-water vapour environment a) 750 °C b) 650 °C c) 550 °C d) 450 °C

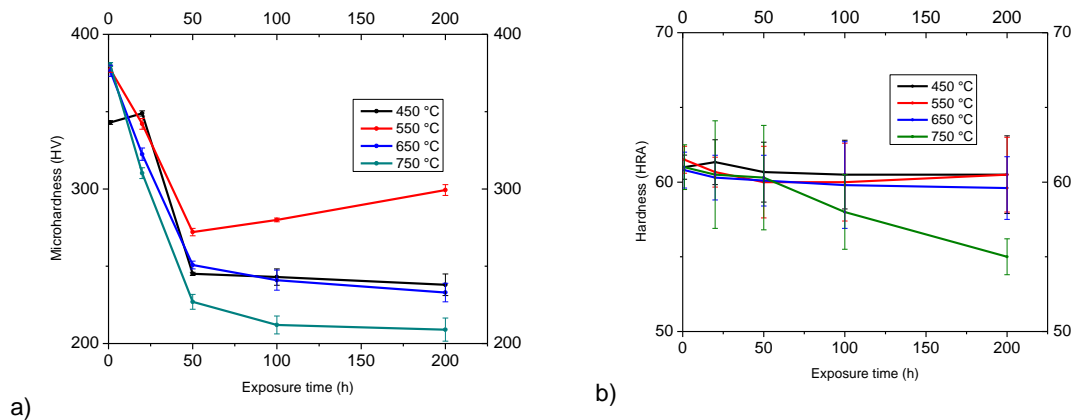


Figure 3: a) Microhardness of ASTM A335 P92 steel after exposure to oxidation- water vapour environment b) Hardness of ASTM A335 P92 steel after exposure to oxidation- water vapour environment

### 3.2 Oxidation-nitridation-water vapour environment

In Figure 4, it is possible to observe that by exposing the steel to the temperatures of 750 and 650 °C, the tempered martensitic structure tends to transform into a ferritic matrix. Similarly, the precipitation of metal carbides of elements such as W, Mo, V, Nb, and Fe within the ferritic matrix and formation of metal oxides is evident. For the temperature of 750 °C, it is possible to observe a greater globulisation of the carbides formed. The micrographs observed at the temperatures of 550 °C and 450 °C show an acicular tempered martensitic microstructure in the material that tends to transform into a ferritic matrix, where the formation of metal oxides and carbides within the steel structure can be observed.

Figure 5a shows the behaviour of the microhardness in the material for the four working temperatures. It is possible to observe slight variations for the temperatures of 450 °C, 550 °C and 650 °C. For the temperature of 750 °C the behaviour presents a linear tendency, reaching its lowest value after 200 h of exposure (318 HV).

This initial increase in microhardness is mainly due to the precipitation of carbides. However, due to the effect of temperature and exposure time, a decrease is observed, which is mainly attributed to the effect of temperature, allowing the tempered martensite structure present in ASTM A335 P92 steel to transform into a ferritic matrix.

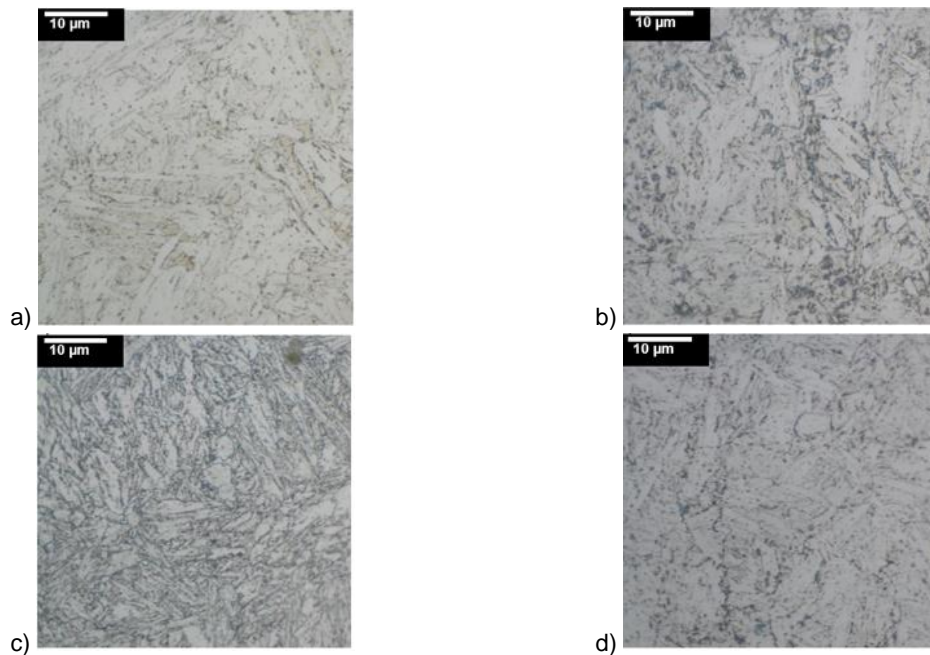


Figure 4: Micrographs of ASTM A335 P92 steel after 200 h of exposure to oxidation-nitridation-water vapour environment a) 750 °C b) 650 °C c) 550 °C d) 450 °C

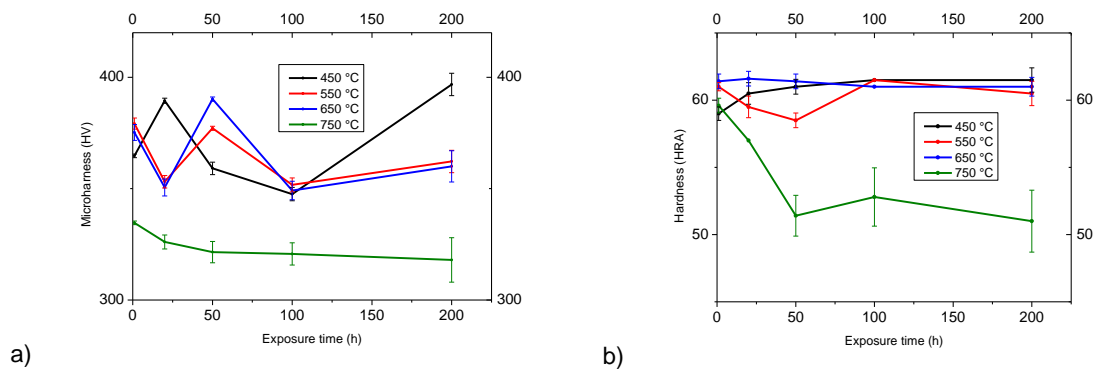


Figure 5: a) Microhardness of ASTM A335 P92 steel after exposure to oxidation- water vapour environment b) Hardness of ASTM A335 P92 steel after exposure to oxidation-nitridation-water vapour environment

The observed behaviour is similar to that presented for the oxidation-water vapour environment, where the material for the working temperatures of 450, 550 and 650 °C do not show a significant variation (Figure 5b). However, for the temperature of 750 °C, a decrease is observed to a value of 51 HRA, which is mainly due to exceeding the maximum working temperature (620 °C), the steel undergoes microstructural changes, which it causes a tendency of change of the tempered martensitic structure in the steel to a ferritic matrix, leading to a decrease in the hardness of the material.

#### 4. Conclusions

In this work, the effects of corrosive environments oxidation, nitridation, water vapour in ASTM A335 P92 steel were studied in order to observe the changes in the structure of the material, in addition, to analyze the changes on the microhardness and hardness of the steel at different temperatures. It was observed that due to the effects of temperature, the tempered martensitic structure tends to transform into a ferritic matrix with carbide precipitation. For all working temperatures and exposure time of 1h, an increase in microhardness was observed, mainly due to the precipitation of carbides. Depending on the exposure time and operating temperature, a decrease in the microhardness of the steel is evident, especially for the temperature of 750 °C, the steel increases the speed of the diffusive processes, which allows decreasing the carbon content distributed homogeneously in the matrix. Although the presence of carbides and oxides was visible visually, due to their globulisation, it is suggested for future investigations to characterise these by means of characterisation techniques.

#### Acknowledgements

The authors expressed their acknowledgments to COLCIENCIAS and RECIEE, for financial support of this work that is part of the project "Consolidation of the knowledge network on energy efficiency and its impact on the productive sector under international standards - Design of a methodology for the eco-efficient management of combustion processes, case study: the oil refining industry" code of COLCIENCIAS: 110154332086.

#### References

- ASTM, A. A. N. S., 1995, Standard practice for preparation of metallographic specimens (E3-95), Annual Book of ASTM Standards, 3, 1–9.
- ASTM., 2015, E407 – 07e1: Standard Practice for Microetching Metals and Alloys, ASTM, 1–21.
- ASTM Standard G1-03., 2011, Standard practice for preparing, cleaning, and evaluating corrosion test specimens, ASTM International, West Conshohocken, PA, USA.
- Carrizo D., Besoky J., Luppo M., Danon C., Ramos C., 2018, Characterization of an ASTM A335 P91 ferritic-martensitic steel after continuous cooling cycles at moderate rates. *Integrative Medicine Research*, 8, 923–934.
- Gil De Fuentes L., 2013, Corrosion in the oil industry and the use of coating technologies as a protection alternative <ciencias.uis.edu.co/imrmpt/resumenes/Resumen%20Linda%20Gil%202nd%20IMRMPT.pdf> accessed 24.07.2019. (In Spanish).
- Gond D., Chawla V., Puri D., Prakash S., 2010, Oxidation Studies of T-91 and T-22 Boiler Steels in Air at 900 °C, *Journal of Minerals & Materials Characterization & Engineering*, 9, 749–761.
- Kafarov V., Toledo M., Meriño L., 2015, Numerical simulation of combustion process of fuel gas mixtures at refining industry, *Chemical Engineering Transactions*, 43, 1351–1356.
- Orozco J. C., Kafarov V., Pena D. Y., Alviz A., 2017, Effects of oxidation-nitridation in the presence of water vapor on ASTM A335 P92 steel using SEM-EDS and XPS characterization techniques, *Journal of Physics: Conference Series*, 935, 1-7.
- Orozco J., Kafarov V., Peña D., 2018, Methodology for the Analysis of ASTM A335 P92 Steel Exposed to Real Atmospheres of Refinery Combustion. *Chemical Engineering Transactions*, 70, 163–168.
- Peña B., Estupiñán H., Chacón J., Infanzon D., 2014, Oxidación A Alta Temperatura De Un Acero ASTM A335 P92 En Condiciones Isotérmicas Y De Ciclado Térmico, *Revista Fuentes*, 12, 5–13.
- Peña-Ballesteros D., Vásquez-Quintero C., Laverde-Cataño D., Serna G A., 2012, Corrosión a temperatura alta del acero ferrítico 9Cr-1Mo modificado P91, en atmósferas simuladas oxidantes-carburantes. *Revista de Metalurgia*, 48, 97–106.
- Young D. (Ed), 2016, High Temperature Oxidation and Corrosion of Metals, Elsevier Corrosion Series, Cambridge, UK.